

Characteristic X-ray Production in Thin Crystals

D. Cherns and A. Howie

Cavendish Laboratory, Cambridge, England

and M. H. Jacobs

Tube Investments Research Laboratories, Hinxton Hall, Saffron Walden, England

(Z. Naturforsch. **28 a**, 565–571 [1973]; received 1 February 1973)

Dedicated to Prof. Dr. G. Borrmann on the occasion of his 65th birthday

The dependence of the characteristic X-ray production on electron beam orientation is studied using very thin epitaxially grown single crystals. In crystals of Ag and Pd of thickness ~ 100 Å the L shell yield can change by more than a factor of 2 for small changes in orientation near the [111] direction. Theoretical analysis of the results shows that the different Bloch waves do not produce X-rays independently but that interference effects occur. The significance of these observations is discussed.

Introduction

The Borrmann effect, first observed¹ as an anomalously high penetration of X-rays in perfect crystals oriented close to the Bragg position and explained by von Laue² with reference to the standing wave patterns of the Bloch wave intensities, has had important repercussions in electron diffraction. In particular, similar anomalous transmission effects were observed in electron diffraction patterns^{3, 4, 5} and were shown to be of importance in understanding many features of the electron micrographs of both perfect and imperfect crystals^{6, 7, 8}. Electron microscopy of relatively thick crystals is indeed only a practical possibility because of the Borrmann effect and the phenomenological theory developed to explain the observations is qualitatively quite similar to that used for X-rays.

Despite these similarities, the inelastic scattering processes which effectively attenuate the beam are quite different for electrons and have required more detailed calculation^{9, 10} than in the X-ray case where the photo-electric effect predominates. The related process of inner shell ionisation is by comparison relatively unimportant as a cause of attenuation in electron diffraction but can however be conveniently monitored by measuring the intensity of characteristic X-rays which result. As pointed out by Hirsch et al.¹¹, the X-rays produced by an electron beam falling on a crystal might therefore be expected to show a Borrmann effect i.e. a dependence on the

orientation of the incident beam relative to the crystal and this was indeed observed by Duncumb¹² using an early form of combined electron microscopy and X-ray microanalysis equipment EMMA I. The phenomenon was subsequently investigated in more detail by Hall¹³, who showed that it was only of importance in comparatively thin crystals of thickness $t \lesssim 2000$ Å, the characteristic attenuation distance of the poorly transmitted Bloch waves which produce most of the X-rays. At greater distances from the entrance surface the electrons have been diffusely scattered through small angles and effectively behave like plane waves in producing further X-rays.

The Borrmann effect in X-ray production is thus of considerable potential importance in quantitative X-ray microanalysis particularly when very thin well oriented crystals are used. These conditions have not in fact applied in most microanalysis work carried out to date but it may be expected that they will be approached more closely in the future as high resolution microanalysis of thin films becomes more practical, particularly with the advent of high intensity, transmission scanning electron microscopes.

In the present work it has proved possible to examine the details of the Borrmann effect in extremely thin crystals grown epitaxially on thin film crystalline substrates of a different material. The results presented below show the great importance of the orientation effect in the X-ray production and the need to take account of it if reliable estimates of the thickness of the overgrowth or of the composition of the overall film are to be obtained by X-ray microanalysis techniques.

Reprint requests to Dr. A. Howie, Cavendish Laboratory, Cambridge/England.



Dieses Werk wurde im Jahr 2013 vom Verlag Zeitschrift für Naturforschung in Zusammenarbeit mit der Max-Planck-Gesellschaft zur Förderung der Wissenschaften e.V. digitalisiert und unter folgender Lizenz veröffentlicht: Creative Commons Namensnennung-Keine Bearbeitung 3.0 Deutschland Lizenz.

Zum 01.01.2015 ist eine Anpassung der Lizenzbedingungen (Entfall der Creative Commons Lizenzbedingung „Keine Bearbeitung“) beabsichtigt, um eine Nachnutzung auch im Rahmen zukünftiger wissenschaftlicher Nutzungsformen zu ermöglichen.

This work has been digitalized and published in 2013 by Verlag Zeitschrift für Naturforschung in cooperation with the Max Planck Society for the Advancement of Science under a Creative Commons Attribution-NoDerivs 3.0 Germany License.

On 01.01.2015 it is planned to change the License Conditions (the removal of the Creative Commons License condition “no derivative works”). This is to allow reuse in the area of future scientific usage.

Hall's theory of X-ray production in thin crystals¹³ was somewhat different than the earlier one of Hirsch et al.¹¹ and assumed that different Bloch waves could be treated independently in creating X-rays. Our results are analysed below in order to provide information on this basic theoretical question.

Experimental Details and Results

The type of specimen used in this investigation is shown in Figure 1. The first crystal I was in all cases (111) Au prepared by the method of Pashley¹⁴; Ag was evaporated on to cleaved muscovite mica at 270 °C followed by Au at 150 °C, the Au

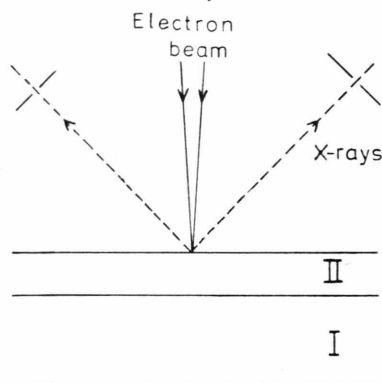


Fig. 1. Arrangement for electron irradiation of the composite crystal and collection of characteristic X-rays.

being detached by dissolving the Ag layer away in 50% nitric acid. The second crystal II of Cu, Pd or Ag was then deposited to a controlled thickness t_{II} , in the range 10–400 Å, measured by a quartz crystal oscillator, good epitaxial conditions being achieved in all cases. Crystal II is also in (111) orientation and grows with an initial pseudomorphic stage but, as it thickens, interfacial dislocations may be generated to relieve the elastic strain. In the case of the Cu and Pd overgrowths, where the misfit is 13% and 5% respectively, this occurs at a few Å thickness. An example of the dislocation network subsequently formed is shown in Figure 2*. In the case of Ag the misfit parameter is much smaller (0.2% difference in lattice parameter) and interfacial dislocations were seldom observed in the films used. The generation mechanisms for interfacial dislocations will be described elsewhere.

The composite films were then examined in the EMMA III combined electron microscopy and X-ray microanalysis equipment¹⁵, operating at 100 keV. In this machine the beam can be focused

to a spot of about 1000 Å diameter on the specimen surface and the X-rays emitted from the irradiated region of the specimen detected by two crystal spectrometers. These have collection solid angles of approximately 2×10^{-2} sterad and detect X-rays emitted in the backward direction at about 135° to the incident electron beam as shown in Figure 1. In our investigations CuK_α , PdL_α , AgL_α and AuL_α were detected, count rates being in the range 5 to 250 per second with a probe size of about 2000 Å and a probe current of 5×10^{-8} Amps.

The exact position of the probe on the specimen and the precise crystallographic orientation of the film in the irradiated region can, of course, be obtained by reference to the electron micrograph. Figure 3 shows the position and size of the probe relative to the extinction contours near a (111) orientation and it can be seen that the crystal is sufficiently flat for regions of approximately constant orientation to be selected.

The range of crystal orientations selected is also affected by the appreciable beam divergence associated with a small focused probe. Under the operating conditions (250 μ condenser aperture, 2000 Å probe) the beam divergence was nearly equal to the Bragg angle for 220 reflections. The effect of reducing this by employing smaller condenser apertures and slightly increasing the probe size, thus reducing the divergence by a factor of up to 10, was investigated on a 35 Å Pd/Au film. No significant changes were observed, although in retrospect a rather insensitive part of the curve (see Fig. 4) was chosen and it would be useful to repeat this type of experiment on thicker films.

For any specimen the appropriate *K* or *L* shell emission from crystal I or II could be detected at each desired crystal orientation. As expected from the results of Hall¹³, noted above, the X-ray output from crystal II usually showed much more sensitivity to the crystal orientation than the output from crystal I. The difficulty of performing microanalysis measurements, i. e. of determining the relative thickness of the two crystals by comparison of the two X-ray signals is thus clear. The point was made more dramatically by comparing the signals obtained with the sample, as shown in Figure 1, with those obtained when it was turned upside down. In this case a further effect arises because of the attenuation of the X-rays from the lower crystal in passing through the upper crystal. The attenuation distance of AgL_α X-rays in Au, for instance, is about 3000 Å so that the influence of this effect can be considerable. Some selected results, indicating the difficulty of microanalysis in composite films of this kind, are given in Table 1.

* Figures 2 and 3 on page 568 a.

Tab. 1. Effect of Tilting or Inverting the Specimen on X-ray Count Ratio.

Film		Overgrowth counts II		Au counts I		Count ratio II : I	
		Position 1	Position 4	Position 1	Position 4	Position 1	Position 4
80 Å Ag/1000 Å Au	(a)	24244	11967	21421	19955	1.13 ± 0.02	0.60 ± 0.01
	(b)	10590	7556	26054	22473	0.41 ± 0.01	0.34 ± 0.01
300 Å Cu/200 Å Au	(a)	9998	6734	5874	5285	1.70 ± 0.05	1.27 ± 0.05
	(b)	6390	5539	5748	4091	1.11 ± 0.04	1.35 ± 0.05
600 Å CuAu alloy		3493	2914	8213	6825	0.43 ± 0.02	0.43 ± 0.02

(a) refers to Au underneath as in Fig. 1, (b) refers to Au on top. Positions 1 and 4 of the probe are shown in Figure 3. All tabulated counts were the sum of three 100 sec counts.

The dependence of the X-ray output from crystal II on orientation, was investigated in detail for Pd and Ag layers of various thickness t_{II} in the range 10 Å to 100 Å for Pd and 10 Å to 350 Å for Ag on top of Au crystals I of thickness t_I typically about 1000 Å. Measurements were made at 4 different orientations, (1) at the (111) pole (6 reflections of 220 type equally but not exactly excited); (2) at the exact Bragg position for a single (220) reflection; (3) at the systematic symmetry position mid-way between the (220) and (220) reflections; and (4) at a general position well away from any strong Bragg reflections. It was confirmed that near position (4) the output was quite insensitive to orientation and the reproducibility of the results in the other positions was checked by repeated experiments. The various probe positions referred to are indicated in Figure 3. It was also checked that at constant orientation the X-ray output did not vary significantly from point to point, so that it could be assumed that the thickness of the two crystals was reasonably uniform.

Of the positions (1), (2) and (3) a marked enhancement of the X-ray count was found at position (1), compared with that at (4), with a slight enhancement at position (3), and no significant effect at (2). The results shown in Fig. 4 give the ratios of three 100 sec. counts at position (1) compared with three at position (4) for each Pd/Au and Ag/Au film investigated. The approximate counts for the 300 sec. period were about 10,000 at position (4) for both the 100 Å Pd/Au and Ag/Au films. The ratios of isolated 100 second counts at positions 3 and 4 are shown in Figure 5. The errors, indicated in the Figs. 4 and 5 for Ag only, are $2 \cdot N^{\frac{1}{2}}$ where N is the number of counts involved including background.

X-ray microanalysis of the Au crystals alone showed that there was no detectable contamination as a result of alloying with the initial Ag film used in their preparation.

Theoretical Analysis

The ionisation of inner shell electrons is a process which makes a small contribution to the imaginary part of the crystal potential $iV'(\mathbf{r})$ and this could be calculated following Whelan¹⁶ from a knowledge of the relevant wave functions. These calculations would be rather laborious however, particularly in the case of heavy atoms, since it is unlikely that the exchange terms could be neglected. Since the absolute magnitude of the effect is unimportant for our present purpose we have simply assumed that the relevant part of the imaginary potential i.e. the region of X-ray production is approximately a delta function at each atomic site broadened only by the thermal vibrations so that it has Fourier components P_g given by

$$P_g = P_0 \exp\{-\alpha g^2\} \quad (1)$$

where α is the usual Debye Waller factor and P_0 is an arbitrary constant. This assumption is made plausible by the fact that the radius of the L shell in Ag and Pd is about 0.08 Å i.e. considerably less than the thermal vibration amplitude.

The presence of an imaginary potential $iV'(\mathbf{r})$ in the Schrödinger equation can readily be shown¹⁷ to give rise to a rate of loss of electrons per unit volume at the point \mathbf{r} proportional to $V'(\mathbf{r})|\psi(\mathbf{r})|^2$ where ψ is the (total) electron wave function. The X-ray production in a crystal is thus given by

$$X = \int |\psi(\mathbf{r})|^2 \sum_g P_g \exp\{2\pi i \mathbf{g} \cdot \mathbf{r}\} d\tau \quad (2)$$

where the integral extends over the volume of the crystal.

We may express the wave function ψ in the usual way⁸ as a linear combination of Bloch waves whose amplitudes attenuate with increasing depth z in the crystal because of anomalous absorption effects i.e.

$$\psi(\mathbf{r}) = \sum_j \psi^{(j)} \exp\{-2\pi q^{(j)} z\} \sum_g C_g^{(j)} \exp\{2\pi i(\mathbf{k}^{(j)} + \mathbf{g}) \cdot \mathbf{r}\}. \quad (3)$$

For simplicity we assume that the crystal is centrosymmetric so that the Bloch wave elements $C_g^{(j)}$ and excitation amplitudes $\psi^{(j)}$ may be taken to be real. From a crystal of unit area and thickness t , we thus obtain an X-ray output $X_1(t)$ due to Bloch waves and given by the expression

$$X_1(t) = \sum_{j,l} \psi^{(j)} \psi^{(l)} P^{jl} \int_0^t \exp\{-2\pi(q_{jl} - i\Delta k_{jl})z\} dz \quad (4)$$

$$\text{where } \Delta k_{jl} = k_z^{(j)} - k_z^{(l)}, \quad q_{jl} = q^{(j)} + q^{(l)} \quad (5), (6)$$

$$\text{and} \quad P^{jl} = P^{lj} = \sum_{g,h} C_g^{(j)} P_h C_{g-h}^{(l)}. \quad (7)$$

The quantity $P^{jj} = P^{(j)}$ may be regarded as the rate of X-ray production characteristic of each Bloch wave j .

The decrease in the Bloch wave intensities is compensated and indeed caused by an increase in the intensity of electrons diffusely scattered through fairly small angles. Following Hall¹³ we assume that these diffusely scattered electrons behave as plane waves in producing a further contribution $X_2(t)$ to the X-ray output *

$$X_2(t) = P_0 \int_0^t \left(1 - \sum_j |\psi^{(j)}|^2\right) \exp\{-4\pi q^{(j)} z\} dz \quad (8)$$

The total X-ray production may then be written in the form

$$X(t) = P_0 t \left[1 + \sum_j \frac{|\psi^{(j)}|^2 (P^{(j)} - P_0)}{4\pi q^{(j)} P_0 t} (1 - \exp\{-4\pi q^{(j)} t\}) + \sum_{\substack{j,l \\ j \neq l}} \frac{\psi^{(j)} \psi^{(l)} P^{jl}}{2\pi q_{jl} P_0 t (1 + a_{jl}^2)} (1 - \exp\{-2\pi q_{jl} t\}) \{\cos(2\pi \Delta k_{jl} t) - a_{jl} \sin(2\pi \Delta k_{jl} t)\} \right] \quad (9)$$

$$\text{where} \quad a_{jl} = \Delta k_{jl} / q_{jl}.$$

This expression contains the average contribution expected from non-crystalline material, a contribution from individual Bloch waves acting independently and a contribution involving the interference between different Bloch waves. Graphs of $X(t)/P_0 t$ are shown in Fig. 4 for the exact 111 orientation in Ag (a thirteen-beam computation). It may be noted that $X(t) \rightarrow P_0 t$ in thick crystals as expected since the Bloch wave amplitudes then become small. The effect of the interference terms between different Bloch waves is mainly noticeable in very thin crystals as can be seen by comparing the curves computed with and without these terms (see Figure 4). When the interference terms are included it is found that $X(t) \rightarrow P_0 t$ at very small values of t instead of attaining the rather high values predicted by the theory in the absence of these terms. This result is clearly in better agreement with the experimental observations and is indeed intuitively more reasonable since it is difficult to see how in the limit of a

very thin crystal the orientation can be significant. The interference terms also tend to produce slight oscillations at greater thicknesses but it is doubtful whether these could in practice be observed. Thirteen beams were used in the calculation which shows an effect roughly 20% larger near $t_{II} = 100 \text{ \AA}$ than was obtained in preliminary calculations using only seven beams. The difference between the two calculations was much smaller for larger values to t_{II} .

In thicker regions of the crystal the experimental results obtained lie significantly below the theoretical curve of Figure 4. This is certainly due to the rather large angular spread in the probe mentioned above. An attempt to allow for this effect was made by calculating curves of X-ray production for a number of beam directions deviated from [111] by up to the 220 Bragg angle. From the condenser aperture used and also the size of the enlarged spots in the diffraction pattern it was estimated that this corresponded roughly to the angular range in question. A uniform two dimensional average over this range yielded the curve shown in Fig. 4 which is clearly in rather better agreement with the observations. To the accuracy involved here it is not expected that the curves for Ag and Pd would be very different and separate computations have not

* The evidence from Kikuchi bands in fact suggests¹⁸ that after diffuse scattering from Bloch waves with $P^{(j)} > P_0$, there will be some tendency for the X-ray production rate to remain anomalously large. Some account of this could perhaps be taken in the theory given here by using for these Bloch waves rather lower values of $q^{(j)}$ than indicated by transmission experiments.



Fig. 3. Extinction contours near the $[111]$ direction in a specimen consisting of 1000 \AA of Au plus 200 \AA of Ag. The various orientations 1, 2, 3 and 4 referred to in the text are shown and the circles at these points denote the probe size used. In practice these where selected by reference to the diffraction pattern with the probe focussed.

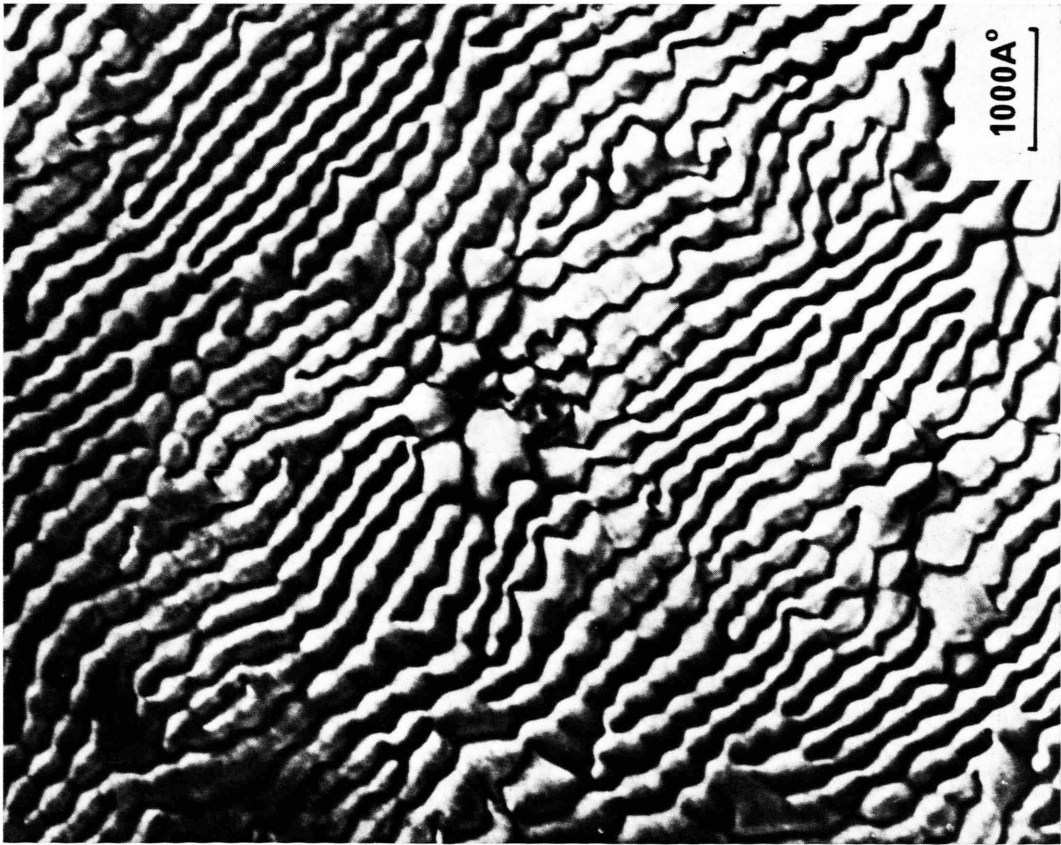


Fig. 2. Hexagonal network of edge dislocations in the interface between a 1400 \AA Au crystal I and a 10 \AA Pd crystal II.

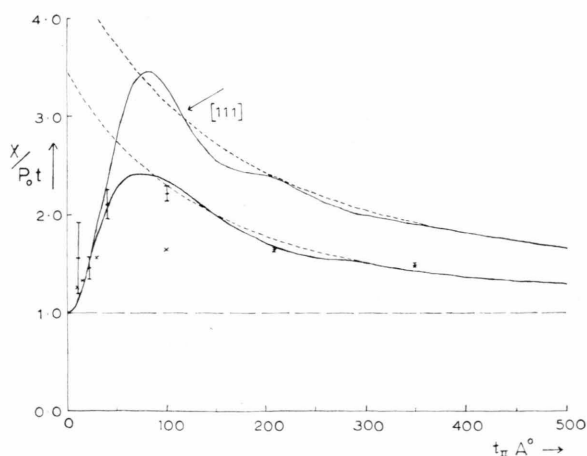


Fig. 4. Comparison between experimental results for the count ratio at positions 1 and 4 (+ refers to Ag/Au films, x to Pd/Au films) and values of $X(t)/P_0 t$ computed from Eqn. (9) represented by full line curves. The broken line curves refer to the independent Bloch wave model. The upper pair of curves are for the exact [111] direction, the lower pair obtained by averaging over an angular range corresponding to the electron probe used.

been done. With a more parallel incident beam however it might be possible not only to approach the ideal curve more closely but also to detect the influence of the interfacial dislocations in the case of the Pd film since they might be expected to reduce the magnitude of the orientation effect.

A further uncertainty arises as to the precise temperature in the irradiated region. Computations were made with a number of different values of the Debye-Waller factor [Eq. (1)] and these indicated that even if the temperature were to rise to 200 °C the reduction in the X-ray production orientation effect would not be significant in comparison with the reduction due to angular spread discussed above.

Figure 5 shows computations of X-ray production made using the systematic 220 reflections with beam orientations corresponding to points 2 and 3 (the exact Bragg position and the symmetry position respectively) in Figure 3. The experimental results for position 3 again fall somewhat below the theoretical curve but calculations made for nearby orientations suggest that, as before, this can probably be explained in terms of the angular spread in the electron probe. Clearly the X-ray anomaly is a good deal less pronounced in this planar channelling situation than in the axial situation of Figure 4. At the Bragg position 2 the experiments did not show any significant result most probably because

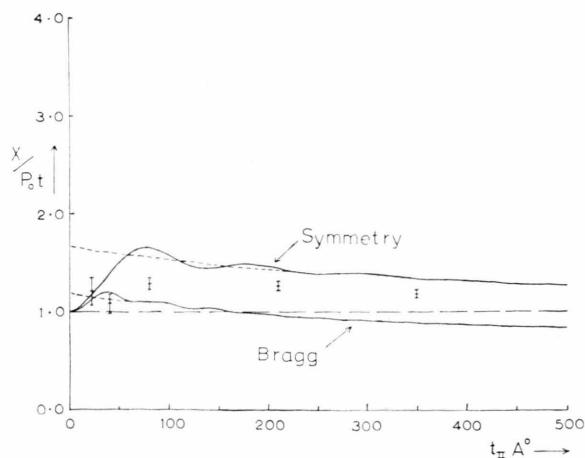


Fig. 5. Comparison between the experimental results for the ratio of counts in Ag/Au films at position 3 to position 4 with computed results. The full lines refer to the theory including interference terms, the broken lines are for the independent Bloch wave model. The upper curves are for the symmetry position 3, the lower pair for the Bragg position 2.

the effect varies rather rapidly with orientation in this region. The theoretical curve shows that for larger values of t_{II} the X-ray production falls below the random value. This is because of the continuing presence of a well transmitted Bloch wave with a very low rate of X-ray production. In still thicker crystals the curve should return to the random level.

Some preliminary calculations were also carried out for the [100] and [110] directions, again using thirteen beams. The curves shown in Fig. 6 are rather similar in form to those for [111] but the magnitude of the effect is significantly less. The

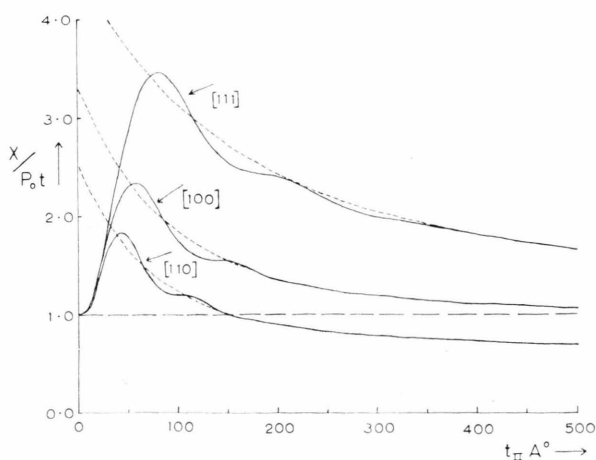


Fig. 6. Computed curves of $X(t)/P_0 t$ for the [111], [110] and [100] directions in Ag using Eqn. (9) (full line curves) and the independent Bloch wave model (broken lines).

Bloch wave which produces X-rays most efficiently is less strongly excited than in the [111] orientation. In all these orientations the X-ray production is probably very sensitive to many-beam effects and there may be a significant dependence on the accelerating potential used.

Discussion

Thin films epitaxially deposited on crystalline substrates are evidently quite useful specimens for studies of the X-ray production effect. In very thin crystals $t_{II} \approx 50 \text{ \AA}$ where the sensitivity to crystal orientation and beam divergence is not acute, the results show quite definitely that the X-ray production should be calculated from the total wave function and not from independent Bloch waves. In thicker crystals $t_{II} \geq 100 \text{ \AA}$ the two theories are not significantly different.

The case for the independent Bloch wave model was originally argued by von Laue² but is only really valid in the case of infinite crystals with zero absorption. The point is also relevant to the theory of electron back-scattering from crystals where for instance some authors^{19, 20} have used the independent Bloch wave model and others^{21, 22} have included the interference terms between different Bloch waves. In particular Reimer et al.²² have used an expression equivalent to Eq. (9) in their back scattering calculations. Since it now appears from the work reported here that the independent Bloch wave model is incorrect, it would be desirable to recalculate the back-scattered electron images of lattice defects including the interference terms. Preliminary results obtained by Clarke (private communication) indicate that, at least in the two beam case near the Bragg position, the resulting modification to the images is quite small.

The question now arises as to whether a similar modification should be made to the anomalous transmission theory of electron diffraction where once again the model widely used⁸ is of Bloch waves which are independently scattered and absorbed. It can readily be shown in this case however that the general solutions to the Schrödinger equation with a periodic complex potential will always consist of linear combinations of independent solutions of the Bloch wave type, each of which has a characteristic wave vector with real and imaginary parts which do not depend on the presence of other Bloch waves.

There is however a small modification to the Bloch wave elements $C_g^{(j)}$ in Eq. (3) because of the presence of the imaginary part of the potential and this is usually ignored on the grounds that in thick crystals it is the attenuation of the waves which is the dominant effect. In thin crystals where the attenuation of the waves is small, the modification of the Bloch wave amplitudes may be more significant however and will produce a change in the transmitted intensities which is periodic with crystal thickness and may be analogous to the effect of the interference terms in the X-ray production problem. For a fully consistent theory of transmission, X-ray production or back-scattering it may therefore be necessary to use the exact Bloch wave elements $C_g^{(j)}$. This involves diagonalisation of a complex non-Hermitian matrix. Alternatively the solutions can be built up by integration of the coupled equations of dynamical theory⁸ for plane waves in an absorbing crystal.

From the point of view of X-ray microanalysis the results presented here show that the orientation effect can be quite significant particularly in crystals of the order of 100 \AA thick. The count rate is liable to depend quite strongly on the crystal orientation and on the angular spread of the illuminating beam. In most practical situations it should be possible by systematic tilting of the specimen to minimise these difficulties by avoiding orientations where strong Bragg reflections occur. Should this be impossible however the present results indicate that it is quite feasible to compute the necessary correction which may arise because of the orientation effect.

Acknowledgements

We are grateful to the S.R.C. for a research grant supporting the epitaxy work in the Cavendish Laboratory and for a CAPS award. The account of the work at Tube Investments Research Laboratories is published by permission of Dr. D. W. Pashley F.R.S. and we are grateful to him for the experimental facilities made available and for his advice on the manuscript. We thank Miss P. L. Gai for assistance in the computations.

Note added in proof: A recent measurement of $X/P_0 t$ at the [111] pole in the case of a 200 \AA film of Ag has shown that the ratio rises from $1.67 \pm .03$ to $1.92 \pm .10$ if the condenser aperture is reduced from 250μ to 100μ .

- ¹ G. Borrmann, Phys. Z. **42**, 157 [1941].
- ² M. von Laue, Acta Cryst. **2**, 106 [1949].
- ³ G. Honjo, J. Phys. Soc. Japan **8**, 776 [1953].
- ⁴ G. Honjo and K. Mihama, J. Phys. Soc. Japan **9**, 184 [1954].
- ⁵ K. Kohra and H. Watanabe, J. Phys. Soc. Japan **14**, 1119 [1959].
- ⁶ H. Hashimoto, A. Howie, and M. J. Whelan, Phil. Mag. **5**, 967 [1960].
- ⁷ H. Hashimoto, A. Howie, and M. J. Whelan, Proc. Roy. Soc. London A **269**, 80 [1962].
- ⁸ P. B. Hirsch, A. Howie, R. B. Nicholson, D. W. Pashley, and M. J. Whelan, "Electron Microscopy of Thin Crystals, Butterworths, London 1965.
- ⁹ C. J. Humphreys and P. B. Hirsch, Phil. Mag. **18**, 115 [1968].
- ¹⁰ G. Radi, Acta Cryst. A **26**, 41 [1969].
- ¹¹ P. B. Hirsch, A. Howie, and M. J. Whelan, Phil. Mag. **7**, 2095 [1962].
- ¹² P. Duncumb, Phil. Mag. **7**, 2101 [1962].
- ¹³ C. R. Hall, Proc. Roy. Soc. A **295**, 140 [1966].
- ¹⁴ D. W. Pashley, Phil. Mag. **4**, 324 [1959].
- ¹⁵ C. J. Cooke and I. K. Openshaw, Proc. IV National Conf. on Electron Microprobe Analysis (Pasadena — Electron Probe Analysis Soc. of America) paper 64 [1969].
- ¹⁶ M. J. Whelan, J. Appl. Phys. **36**, 2099 [1965].
- ¹⁷ R. D. Heidenreich, J. Appl. Phys. **33**, 2321 [1962].
- ¹⁸ C. R. Hall, Phil. Mag. **22**, 63 [1970].
- ¹⁹ D. R. Clarke and A. Howie, Phil. Mag. **24**, 959 [1971].
- ²⁰ J. P. Spencer, C. J. Humphreys, and P. B. Hirsch, Phil. Mag. **26**, 193 [1972].
- ²¹ E. Vicario, M. Pitaval, and G. Fontaine, Proc. 7th Internat. E. M. Conf. (Grenoble) **2**, 211 [1970].
- ²² L. Reimer, H. G. Badde, H. Seidel, and W. Bühring, Z. angew. Phys. **31**, 145 [1971].

Absorption and Penetration in the Semi-classical Theory of High Energy Electron Diffraction

P. A. Doyle and M. V. Berry

H. H. Wills Physics Laboratory, University of Bristol, United Kingdom

(Z. Naturforsch. **28 a**, 571—576 [1973] ; received 22 January 1973)

Dedicated to Professor Dr. G. Borrmann on his 65th birthday

The approximations under which the effect of inelastic scattering on the elastic scattering of electrons can be described by the use of a complex potential are discussed. Within these approximations, inelastic scattering is incorporated in the semi-classical theory for high energy electron diffraction. A simple explanation is given for the voltage and orientation at which maximum penetration is achieved for thick crystals. Good agreement is obtained between the predictions of this semi-classical theory and those of the conventional quantum mechanical approach for gold (111) systematics.

1. Introduction

A number of theories for the dynamical scattering of fast charged particles by crystals have been given¹⁻⁵. Recently, Berry⁶ (hereafter called I) developed a semi-classical approximation for elastic scattering. This treatment becomes increasingly valid at higher accelerating voltages, for which the greater number of interacting beams renders alternative approaches more difficult to handle numerically.

Inelastic scattering has been included phenomenologically in dynamical theories for electrons^{7, 8} by the use of a complex potential. This complex potential gives an account of the phenomenon of Bloch wave channeling, just as the use of a complex structure factor describes the Borrmann effect^{9, 10} for

X-rays. The approximations under which this potential is valid were described by Yoshioka¹¹ and by Radi¹². We make use of the work of these authors to discuss the effect of the inelastic on the elastic scattering of electrons, using the semi-classical theory of I. In this approach the wave functions are studied in real space, which enables an understanding to be obtained of the physical origin of channeling for different Bloch waves; in addition, the method results in simple analytical formulae, and is thus complementary to the conventional many beam computational techniques⁸. Particular attention is paid to an explanation of the voltage and orientation which maximize electron penetration of thick specimens.

2. The Complex Potential in Electron Diffraction

Consider an electron of kinetic energy eE , wave vector \mathbf{k}_0 and relativistic mass m incident on a crystal of volume V , which can exist in excited states n .